NASA TECHNICAL MEMORANDUM

NASA TM-73886

NASA TM-73886

EXPERIMENTAL DETERMINATION OF TRANSIENT STRAIN IN A THERMALLY-CYCLED SIMULATED TURBINE BLADE UTILIZING A NON-CONTACT TECHNIQUE

by Frederick D. Calfo and Peter T. Bizon
Lewis Research Center
Cleveland, Ohio 44135

January 1978

1. Report No. NASA TM-73886	2. Government Accession No.	3. Recipient's Catalog No.
4. Title and Subtitle EXPERIMENTAL DETERMINATION OF TRANSIENT STRAIN IN A THERMALLY-CYCLED SIMULATED TURBINE BLADE UTILIZING A NON-CONTACT TECHNIQUE		5. Report Date January 1978 6. Performing Organization Code
7. Author(s) Frederick D. Calfo and Peter T. Bizon		8. Performing Organization Report No. E-9500 10. Work Unit No.
9. Performing Organization Name and Address National Aeronautics and Space Administration Lewis Research Center Cleveland, Ohio 44135		11. Contract or Grant No.
12. Sponsoring Agency Name and Address National Aeronautics and Space Administration Washington, D.C. 20546		13. Type of Report and Period Covered Technical Memorandum 14. Sponsoring Agency Code

15. Supplementary Notes

16. Abstract

A type of non-contacting electro-optical extensometer was used to measure the displacement between parallel targets mounted on the leading edge of a simulated turbine blade throughout a complete heating and cooling cycle. The blade was cyclically heated and cooled by moving it into and out of a Mach 1 hot-gas stream. The principle of operation and measurement procedure of the electro-optical extensometer are described.

17. Key Words (Suggested by Author(s))	18. Distribution Statement
Turbine blades; Thermal fatigue; Extensometers; Optical measurement; Structural strain; Displacement measurement; Deformation	Unclassified - unlimited STAR Category 39

19. Security Classif. (of this report)	20. Security Classif. (of this page)	21. No. of Pages	22. Price*
Unclassified	Unclassified		

EXPERIMENTAL DETERMINATION OF TRANSIENT STRAIN IN A THERMALLY-CYCLED SIMULATED TURBINE BLADE UTILIZING A NON-CONTACT TECHNIQUE

by Frederick D. Calfo and Peter T. Bizon

Lewis Research Center

E-9500

SUMMARY

A non-contacting technique to experimentally determine strain is described. This technique was used to measure leading edge strain in a thermally cycled simulated turbine blade. The blade was subjected to cyclic heating (3 minutes) and cooling (1 minute) by moving it into and out of a Mach 1 hot gas stream so that metal temperatures ranging from 1370 °K (2000 °F) to 300 °K (80 °F) were obtained. The technique employed a commercially available non-contacting electro-optical extensometer to measure transient displacement between parallel platinum-rhodium wire targets which were mounted on the blade leading edge. The sensing portion of the extensometer system was designed to "track" the blade targets during the complete cycle including the transitions between heating and cooling. Calibration

measurements showed the instrument could measure the displacement to ± 0.04% of the gage length (the distance between the targets). A maximum total strain of 1.27% occurred at the end of heating. After 10 seconds of heating the total leading edge strain was about 80% of the maximum strain. The minimum total strain at the end of cooling was 0.31%. Strain results were reproducible within 4%.

INTRODUCTION

A major goal of the fatigue research being conducted at the Lewis Research Center is the development and evaluation of life prediction methods which would be applicable to aircraft gas turbine engine components such as blades and vanes. A number of papers (refs. 1-7) describe this work. These studies include: (1) development of life prediction methods utilizing laboratory data obtained for a wide range of materials, and (2) evaluation of these methods through a variety of burner rig studies on simulated engine components such as turbine blades.

Life predictions must be made by engine designers prior to the construction of a complex piece of hardware. The basic input for any life prediction analysis is the strain history at the critical location of the component such as the leading edge for many turbine blade configurations. A designer of a turbine blade computes this strain history by

using the geometry, material properties, and an assumed temperature history based on previous experience. Obviously the computed strain history for a turbine blade has in it its own uncertainties and approximations based on the input assumptions. In attempting to verify a life prediction method such as Strainrange Partitioning (SRP) (refs. 1-5), it is important to be able to separate out all possible sources of uncertainties and approximations, so that the "pieces" can be evaluated separately. The ability to measure accurately the strain history at the critical location of the component provides a means of eliminating one of the uncertainties. The measurements such as those of this investigation will permit an evaluation of our ability to compute inelastic strains encountered in a simulated turbine blade subjected to conditions that might occur in an engine. In addition, use of these specific measured strains, along with the characteristic fatigue life relationships (SRP lines) for B 1900 alloy and an appropriate damage rule, should permit us to predict the fatigue life of this simulated turbine blade. Comparison of this predicted life with actual life as determined in a test facility can then be used to provide an indication of the effectiveness of the life prediction method. The application of the measured results reported herein to this life prediction problem is not, however, a part of this report.

Various experimental strain measurement methods currently available are not adequate for obtaining the accurate data needed for this type of investigation which involves high temperatures. For example, temperatures of 1370° K (2000° F) as well as hold time at temperature eliminated consideration of foil or wire strain gages (ref. 8) for the present study. Furthermore, the need to determine strain at the leading edge of the blade eliminated the possibility of applying methods which measure average strain over the cross section such as non-contact capacitance displacement sensors (ref. 9). The requirement that strain be measured for the complete cycle limited the usefulness of extensometer systems capable of measuring strains sensed outside of the hot zone of the specimen (ref. 10). Other non-contacting techniques (refs. 11-13) have been successful in accurately measuring small dimensional changes of a specimen under tension, but have been applied only to static tests.

The purpose of this investigation was to measure the leading edge strain of a simulated turbine blade moving into and out of a hot gas stream. This report presents a detailed description of the experimental measurement method and principle of operation of the commercially available electro-optical extensometer employed as well as the strain data obtained.

The turbine blade studied in this investigation was a

solid, cambered, airfoil design. It was moved into and out of a high velocity hot gas stream to simulate the thermal fatigue loading experienced by blades in aircraft gas turbines. The blade was held in a Mach 1 gas stream for three minutes and then moved out for one minute so that metal temperatures ranging from 1370 °K (2000 °F) to 300 °K (80 °F) were obtained.

The leading edge strain of the simulated turbine blade throughout the cycle was determined in the following manner. Two parallel wire targets were mounted on the leading edge of the blade. A non-contacting electro-optical extensometer measured the displacement (change in length between the targets) throughout the cycle and converted this to an electrical signal which was recorded on a stripchart. The ratio of the displacement at temperature to the distance between the targets at room temperature gave the strain.

This work was conducted using the U.S. customary system of units. Conversion to International System of Units (SI) was made for reporting purposes only.

APPARATUS AND PROCEDURE

Test Specimen

The geometry of the simulated turbine blade is shown in figure 1(a). The blade was precision cast from nickel-base

alloy B 1900. Figure 1(b) shows the blade with the two parallel 0.15 cm (0.060 in.) diameter platinum-rhodium wire targets mounted on the leading edge 1.42 cm (0.561 in.) apart. High temperature braze material was used to fasten the wire targets to the leading edge.

As seen in the cross section of figure 1(a), the airfoil design had its mass concentrated along the mid-chord region. This region controlled the average elongation of the blade, thus restraining both the leading and trailing edges during the thermal cycle. During heating and cooling internal thermal gradients were generated which caused constraints on the expansion and contraction of elements of material by adjacent material elements. In addition, there was an imposed external constraint of the otherwise free thermal expansion and contraction of the blade by the end grips which prevented the blade from warping. These end grips, as shown in figure 1, also permitted application of tensile loading to simulate centrifugal forces.

Test Facility

The facility used for thermal fatigue testing of the simulated turbine blades is shown in figure 2. The schematic in figure 2(a) shows an overall view including the strain sensing instrumentation. Figure 2(b) shows a photograph of the facility and identifies some of the

instrumentation. Figure 2(c) shows a close-up of the specimen with the burner and cooling nozzles. The burner used natural gas fuel. External air-cooling of the test section could be accomplished using the nozzle to the rear of the specimen. However, in the tests described herein, cooling occurred primarily by radiation and conduction through the grips. A hydraulic loading fixture was used to apply tensile loads to the specimen end grips. The burner gas stream operated at Mach 1 velocity with a mass flow of about 0.5 kg/sec (1 lb/sec) at 1590° K (2400° F). The loading fixture was capable of applying a maximum of 89,000 N (20,000 lb) of load to the specimen. A more detailed description of the burner may be found in reference 14.

The specimens were securely clamped to heavy platens riding in large bearing blocks (fig. 2(a,b)) which were connected to the loading fixture. This clamping method prevented the thermal bowing which is usually present in cambered airfoils subjected to thermal loading. It also prevented the airfoil specimen from warping like an unrestrained blade to relieve thermal stress. The large bearing blocks allowed displacement along a line parallel to the leading and trailing edge axes. This was done to stablize the specimen and also to greatly simplify any subsequent stress analyses. The entire loading fixture was pivoted by means of an electrically actuated hydraulic cylinder so as to move the specimen into and out of the

burner stream (shown schematically in fig. 3). In this way, the burner operated at steady-state while the specimen was thermally cycled.

Test Cycle

The simulated turbine blade was cycled by moving it into and out of a Mach 1 burner gas stream operating at 1590° K (2400° F). This temperature was determined using a water cooled thermocouple probe. The blade was moved into the burner gas stream and heated there for three minutes with the leading edge of the specimen at right angles to the burner stream. This was followed by one minute of cooling after the specimen pivoted out of the burner stream. Transfer time between heating and cooling positions was less than three seconds. Blade metal temperatures measured with chromel-alumel thermocouples ranged between 300° K (80° F) and 1370 °K (2000 °F).

Strain Measuring System

A commercially available electro-optical extensometer was applied to experimentally determine the leading edge strain of the simulated turbine blade as it was cycled by moving it into and out of a burner stream. The system is capable of measuring the relative position of two parallel targets that were mounted perpendicular to the leading edge

of the blade. Strain is then determined as the ratio of this relative position or displacement at temperature to the distance between the targets at ambient temperature conditions.

The electro-optical extensometer consists of both optical and electronic components. The optical system consisting of lenses and prisms is used for acquiring, viewing, and producing an optical image of the targets for use by the electronic components. An image analyzer tube in conjunction with other electronic components is used to produce a dc voltage that is directly proportional to the target displacement. A calibration is necessary to determine the proportionality constant between displacement and dc voltage output.

Electro-optical equipment and procedure. - The system employed in this investigation is shown schematically in figure 4. Figure 4(a) shows the overall system consisting of an illumination source for backlighting the targets, an optical head containing the optical and viewing components, and an electronic control module.

Several different target illumination arrangements were investigated, when it was observed that non-uniform lighting of the targets resulted in a linearity error. Non-linear results were avoided by using a reflector-type quartz-iodine lamp operated from a dc power source. The lamp, mounted to

pivot with the test rig, was located along the viewing axis approximately 15 cm (6 in.) behind the targets. Due to space limitations, backlighting was used to illuminate the targets, causing them to appear in silhouette.

The optical head (fig. 4(a,b)) consists of lenses and mirrors together with the image analyzer section. The image analyzer consists of a photomultiplier tube, deflection yoke, and associated electronic circuitry. The optical head was mounted securely to the test frame within the test facility (as shown in fig. 2(a)) remaining focused on the simulated turbine blade during the complete thermal cycle. The mounting fixture was designed to achieve mechanical stability for the optics during the pivoting of the test rig. The optical head was positioned so that the viewing axis intersected near the center of the target plane and was perpendicular to the direction of target change. The distance from the front of the optical head to the targets was about 25 cm (10 in.).

Figure 2(a,b) shows the location of controls, indicator, and connectors mounted on the optical head. The target size and calibrator adjusting knob was used to adjust the instrument to accommodate different target sizes, and simulate target change. The calibrator slide permitted the calibrator dial to be positioned within target range, after which the calibrator locknut was used to retain the set-up. Use of the calibration controls is explained in the

Calibration section of this report. The viewer allows observation to be made through the optical system for aiming the optical head at the targets. The interconnections are used to interconnect the optical head and the electronic modules. The optical head was mounted to a motorized XYZ table to provide a means for positioning the head locally within the test cell, or remotely using the electronic module.

Figure 4(b) schematically shows the optics located in the optical head. The image reducing system provides resolution for measurement of ±5.08 micrometers (±200 microinches) or ±0.04% of a nominal gage length of 1.3 cm (0.5 in.). Lens 1 was used to cause the image of the two backlighted targets to be directed to the prism system. This lens, at a 25 cm (10 in.) working distance from the turbine blade, was able to focus on a field of view of about 1.8 cm (0.7 in.) diameter. The vignette mask eliminated any stray light rays along the optical center line from passing through the optical system. A blue optical filter was included in front of the lens system to remove the black body radiation of the targets and turbine blade at temperatures up to 1370° K (2000° F).

Prisms 1 and 2 are mechanically coupled to each other and to Lens 2 so as to move laterally on the center line axis. The calibrator dial, shown in figure 2(a) measures the lateral motion of the prisms. Prism 3 is fixed. Only

the edges of the target image pass beyond the prism system. Lens 2 maintains the focus of the image as the prisms are moved along the axis. Lens 3 focuses the image on the front face of the photocathode.

Alignment of the optical system with respect to the targets and illumination source was performed as follows: Visual acquisition of the targets was obtained and the targets centered in the field of view using the viewer (fig. 2(a)) in the depressed position. Target centering and focusing was facilitated using the XYZ positioning table. With the viewer depressed, the optical head was aligned so that both targets were overlapped within the field of view as shown in figure 5. It was found that targets of different length aided in the alignment procedure. For best accuracy and to accommodate near maximum target change, the width of the overlapped portion should be about 25% of the total field of view. The width of the target overlapped region may be adjusted by rotating the target size adjusting knob (fig. 2(a)). When the viewer is pulled outward and the correct illumination obtained, a "ready" indicator on the electronic module should light. Lack of such an indication means the target illumination level should be increased.

Internally, the optical head had the capability to compensate if the viewing axis did not intersect the exact center of the target plane. This was accomplished by providing a bias voltage on the deflection yoke to

electronically position the target image on the photocathode ±0.127 cm (±0.050 in.) along the axis of displacement or ±0.25 cm (±0.100 in.) perpendicular to the axis of displacement. The optical portion of the instrument located within the test facility was exposed to an environment of 285-310° K (50-100° F), and 0-95% relative humidity.

Once the set-up and alignment have been completed all operations are performed outside the test facility using the electronic control module (fig. 4(a)). The function of the electronic control module is to provide a voltage that corresponds to the relative position of the targets in the field of view. A differential amplifier accepts the output voltages from the optical head and provides a voltage which is proportional to the relative positions of the targets on the turbine blade. This latter voltage is recorded on a stripchart for the complete test cycle. The electronic module also has position meters for indication of target location with respect to the field of view. Any necessary change in target image location is achieved by observing the position meters and adjusting the optical head by using the electronic module to reposition the XYZ table.

Principle of operation. - This section describes the measuring principle involved in the electro-optical extensometer system. As was noted in the previous section, the optical head contains lenses and prisms which are arranged to produce a superimposed optical image of the

targets in the field of view. This is schematically shown in figure 5 where the overlapped portion of the targets appear as a dark band on a light background when observed through the viewer. The contrast change at the two dark to light boundaries of the band represent double optical discontinuities to the measuring system.

The superimposed target image is focused on the photocathode by a lens. Wherever light falls on the photocathode, electrons are emitted from the inner surface. Thus, an electron image is formed on an aperture plate within the image analyzer tube. An applied electric field accelerates the electron image down the tube and focuses the electron image on the aperture plate. The aperture plate intercepts almost all of the image and only passes the part of the image that falls on the measuring aperture. The photomultiplier, located behind the aperture, sees only that part of the image that passes through the aperture. Thus the current output of the photomultiplier is a linear function of the intensity of a small portion of the optical image.

An oscillator provides a deflecting magnetic field which moves the electron image up and down across the fixed aperture. The oscillator signal current level is proportional to the position of the electron image at the aperature at any given time. A discontinuity detector monitors the output of the photomultiplier tube. The output

of the photomultiplier is sharply changed when a discontinuity sweeps across the aperture. This change in output instantly causes the discontinuity detector to notify logic circuitry that a "boundary" has been "crossed". The logic circuitry interrogates the deflection system as to where the electron image was when the discontinuity was detected. This interrogated signal is presented as an electrical current directly proportional to the position of a target within the field of view. Each of the two discontinuities is sampled in like manner. Each discontinuity current level is updated with a new sample 30,000 times per second--the frequency of the sweep oscillator. The logic circuitry presents the two electrical signals which are proportional to the displacement of each target to a differential amplifier. This amplifier provides an output that is proportional to the differential motion of the two targets. This output can be displayed on any conventional recording instrument. Any additional details concerning the principle of operation of electro-optical displacement gages may be found in reference 15.

Calibration. - The extensometer output provides the relative displacement between the two targets as a function of time. It is necessary to calibrate the system to relate these relative displacements to absolute values. This is done by simulating a target change by using the calibration controls provided on the optical head. After the optical

head is aligned, the targets properly adjusted, and the "ready" indicator light illuminated as detailed in the Equipment and Procedure Description section, the calibration can be performed.

The calibrator dial (fig. 2(a)) provides readout in 0.00025 cm (0.0001 in.) increments of simulated target change. Unlocking the calibrator locking knob and sliding the calibrator dial assembly in the direction away from the targets provides a slight motion (0.0025 cm (0.0010 in.) or less) of the needle. With the needle slightly deflected the calibrator assembly may be locked in position. By turning the target size adjusting crank clockwise and then counterclockwise, any system error resulting from mechanical backlash can be eliminated. Rotating the bezel on the indicator so that the "zero" mark is directly below the needle establishes the optical zero point.

After allowing at least 45 minutes warm-up time for complete thermal stabilization of the electronics, the "zero" potentiometer on the control module can be adjusted to obtain an electrical output of zero. For maximum accuracy, the electrical readout device (DVM, recorder, etc.) should have a resolution of one millivolt or less.

To establish the system gain or scale factor (volts/cm (volt/in.)), the calibrator dial (previously set to zero) should be observed and the target size adjusting crank

rotated counterclockwise to obtain a dial indicator reading of 0.1240 cm (0.0489 in.). This simulates a 0.076 cm (0.030 in.) target size change for this instrument. With this value a dial indicator error no greater than 127 microcentimeters (50 microinches) exists.

With the target change simulated, the "span" potentiometer can be adjusted to provide a convenient output voltage. In this investigation 3.0 volts for the 0.076 cm (0.030 in.) target size change was used. By turning the target size adjusting crank clockwise, and then counterclockwise, the system can again be returned to the optical zero setting. The above steps should be repeated until both the optical and electrical zeros and calibration points are stable and reproducible.

RESULTS AND DISCUSSION

The total leading edge strain for the B 1900 alloy simulated solid turbine blade as a function of time for a typical stable cycle is shown in figure 6. A number of cycles were run and studied for data reproducibility. This study showed that the results were reproducible within 4%. A maximum total strain of 1.27% occurred at the end of heating. After 10 seconds of heating the leading edge strain was about 80% of the maximum strain. The minimum total strain at the end of cooling was 0.31%. The

electro-optical extensometer tracked well as the loading fixture pivoted to move the blade into and out of the burner stream. This is shown in figure 6 by the smooth curve generated as the specimen cycled from heating to cooling. Since the blade was not constrained in the direction of strain measurement, the large strain at steady state reveals that the blade maintained large thermal gradients during this portion of the cycle. Large temperature gradients were indeed observed by using an optical pyrometer and infrared photography of the pressure surface at steady state. These temperature measurement methods showed temperature gradients of over 200° K (300° F) when the leading edge temperature was 1370° K (2000° F).

During an ambient temperature calibration of the extensometer, the system's relative displacement measurement was related to the absolute values obtained by a micrometer. The calibration produced an error no greater than 127 microcentimeters (50 microinches). The displacements during the complete heating and cooling cycle were measured to $\pm$0.04% of the 1.42 cm (0,561 in) gage length.

The data acquisition for the blade specimen was good after a few preliminary problems were resolved. Since the strain measurements were obtained remotely, it was impossible to adjust the instrument set-up during the test. It was therefore, essential to provide a rigidly mounted illumination source since it was required to pivot with the

test rig. Movement of the source during cycling initially illuminated the targets non-uniformly which resulted in linearity errors (output voltage was not linear with displacement). Several lighting arrangements were investigated. Linear results were obtained by using a lamp operating from a dc power source rigidly attached to the test frame.

After determining the optimum operating procedure for the instrument, it was employed with relative ease. The problems normally encountered with more conventional gage methods such as calibration drift or other effects due to severe environmental change, were eliminated since the instrument was external to the test specimen environment.

The results from both the simulated blade measurement as well as the ambient temperature extensometer calibration indicate that it is feasible to use this strain measurement method on other more complicated structures, such as turbine blades containing holes and/or slots for cooling.

CONCLUDING REMARKS

The measurement procedure and the principle of operation of a commercially available non-contacting electro-optical extensometer applied to a simulated turbine blade are detailed. Total leading edge strain resulting

from cycling a solid blade (3 minutes heating and 1 minute cooling) by moving it into and out of a Mach 1 hot gas stream varied between a maximum of 1.27% at the end of heating to a minimum of 0.31% at the end of cooling. Strain results were reproducible within 4%. Metal temperatures of the blade ranged from 300° K (80° F) to 1370° K (2000° F). Approximately 80% of the maximum total strain was obtained after 10 seconds of heating. Displacements during the complete heating and cooling cycle were measured to ±0.04% of the 1.47 cm (0.561 in.) gage length. This strain measurement technique should significantly aid in obtaining the accurate strain measurements needed at critical locations of complicated structures. As such it should prove to be extremely useful in the development and evaluation of a theory for predicting the thermal fatigue life of structural components.

Lewis Research Center
National Aeronautics and Space Administration,
Cleveland, Ohio, DATE
505-01

REFERENCES

1. Hirschberg, Marvin H.; and Halford, Gary R.: Use of Strainrange Partitioning to Predict High-Temperature Low-Cycle Fatigue Life. NASA TN D-8072, 1976.

2. Halford, G. R.; and Manson, S. S.; Life Prediction of Thermal-Mechanical Fatigue Using Strainrange Partitioning. NASA TM X-71829, 1975.

3. Hirschberg, M. H.; and Halford, G. R.: Strainrange Partitioning: A Tool for Characterizing High Temperature Low Cycle Fatigue - Materials Fatigue Test. NASA TM X-71691, 1975.

4. Halford, G. R.; Hirschberg, M. H.; and Manson, S. S.: Temperature Effects on the Strainrange Partitioning Approach for Creep-Fatigue Analysis. NASA TM X-68023, 1972.

5. Halford, G. R.; Hirschberg, M. H.; and Manson, S. S.: Creep Fatigue Analysis by Strain-Range Partitioning. Symposium on Design for Elevated Temperature Environment, ASME, 1971, pp. 12-28. NASA TM X-67838, 1971.

6. Spera, David A.; and Grisaffe, Salvatore J.: Life Prediction of Turbine Components: On-Going Studies at the NASA Lewis Research Center. NASA TM X-2664, 1973.

7. Spera, D. A.; Calfo, F. D.; and Bizon, P. T.: Thermal Fatigue Testing of Simulated Turbine Blades. NASA TM X-67820, 1971.

8. Rohrbach, C.; and Knublauch, K.: Dehnungsmessung mit Messstreifen bei hoken Temperaturen (Strain Measurements with High Temperature Strain Gauges). Materialpruef., vol. 10, no. 4, Apr. 1968, pp. 105-115. (Transl. NLL-CE-TRANS-4971-/9022.09, Natl. Lending Library for Science and Technology, Boston Spa (England).)

9. Harrigill, William T., Jr., and Krsek, Alois, Jr.: Method for Measuring Static Young's Modulus of Tungsten to 1900 K. NASA TN D-6794, 1972.

10. Bush, A. J.: Extensometer for Hot Specimen. J. Instrum. Soc. Am., vol. 11, no. 8, Aug. 1964, pp. 49-50.

11. Sigmon, William, M.: An Optical Extensometer Technique for Strain Measurement. Rep. S-246, Rohm and Haas Co., 1970.

12. Coleman, W. J.: Laser Extensometer. 21st.IISA Annual Conference Proceedings, Vol. 21, Part II, Physical and Mechanical Measurement Instrumentaion. ISA, 1966, Preprint 16.16-3-66.

13. Kharchenko, V. K.; et al.: Device for Measuring Deformations at High Temperatures. Strength Mater., vol. 7, no. 3, Mar. 1975, pp. 376-377.

14. Johnston, James R., and Ashbrook, Richard L.: Oxidation and Thermal Fatigue Cracking of Nickel- and Cobalt-Base Alloys in a High Velocity Gas Stream. NASA TN D-5376, 1969.

15. Starer, Robert, L.: Electro-Optical Tracking Techniques. Instrum. Contr. Syst., vol. 40, no. 2, Feb. 1967, pp. 103-105.

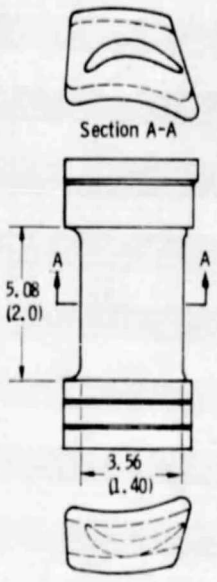

(a) Geometry.

Figure 1. - Simulated turbine blade.
(All dimensions are in cm (in.).)

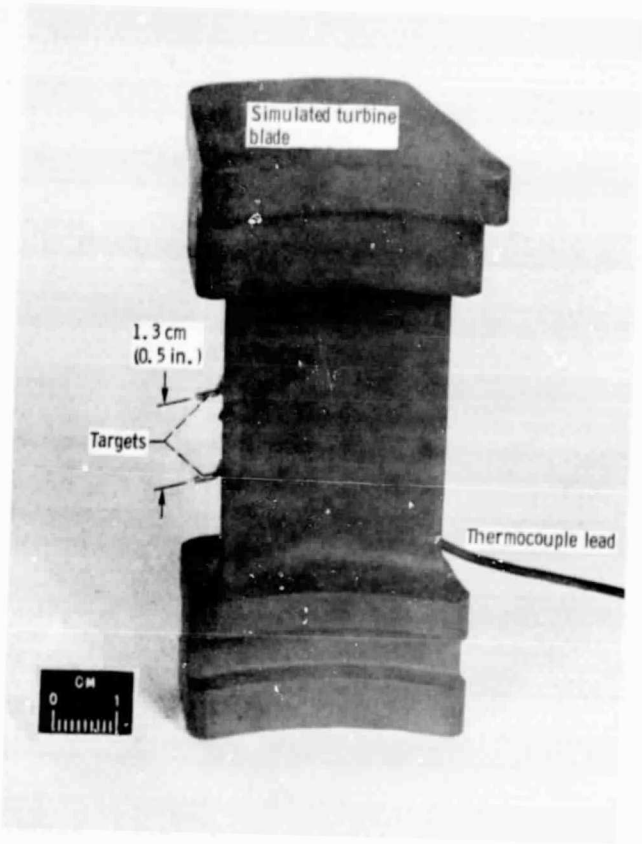

(b) Blade specimen with targets mounted.

Figure 1. - Concluded.

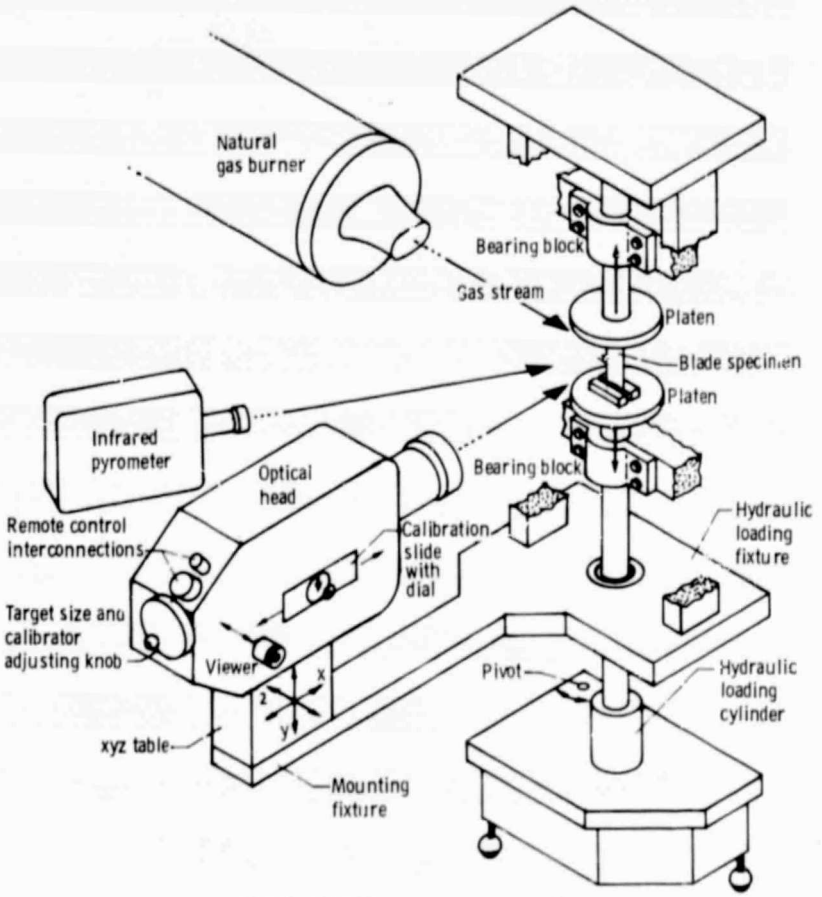

(a) Details of load frame and instrumentation.

Figure 2. - Facility for thermal-fatigue testing of simulated turbine blades.

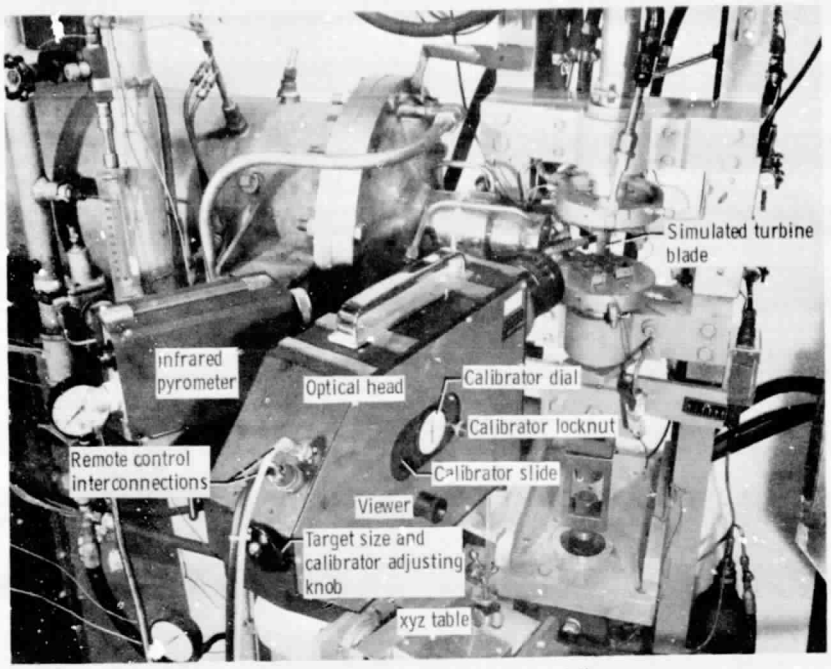

(b) Details of strain sensing instrumentation.

Figure 2. - Continued.

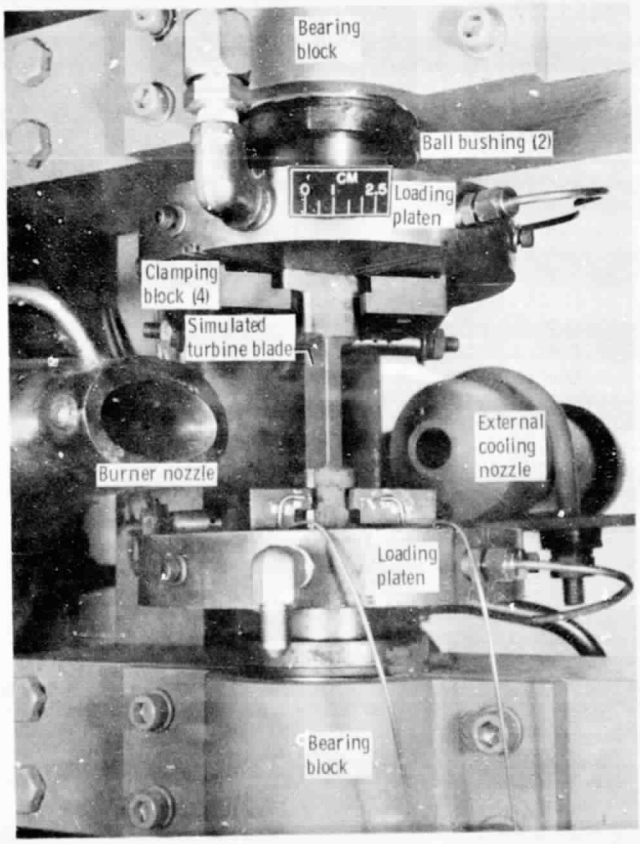

(c) Section of facility showing heating and cooling nozzles; specimen is in heating position.

Figure 2. - Concluded.

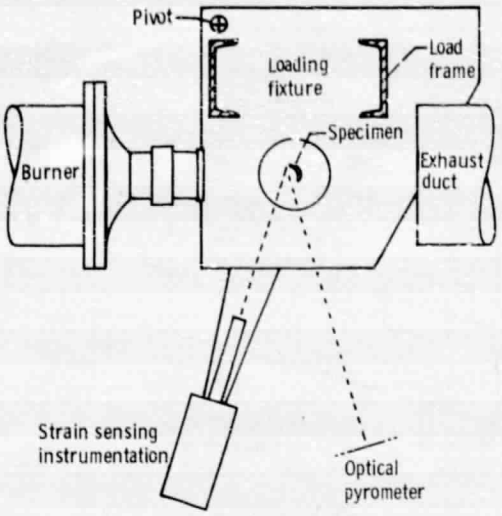

(a) Heating position.

Figure 3. - Schematic of facility showing the specimen located in the heating and cooling positions.

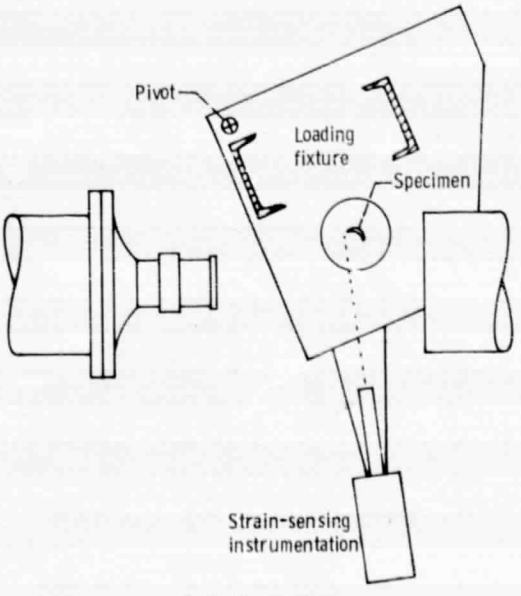

(b) Cooling position.

Figure 3. - Concluded.

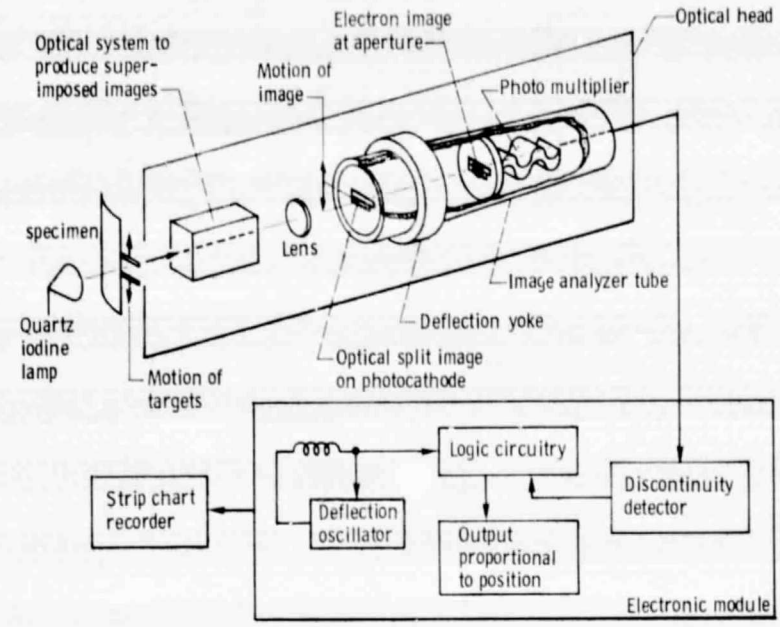

(a) Overall system.

Figure 4. - Schematic description of electro-optical system.

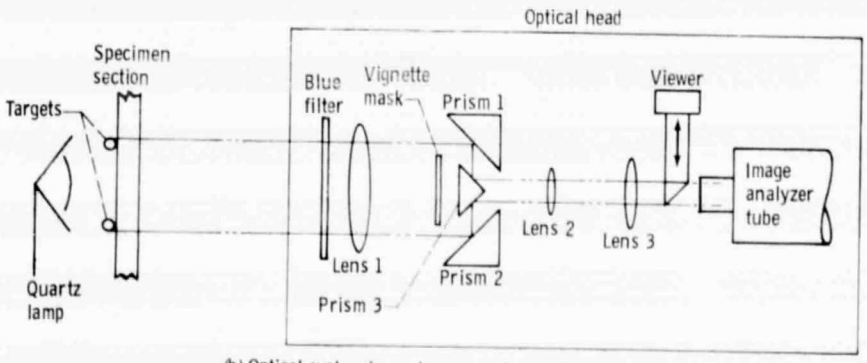

(b) Optical system to produce superimposed images.

Figure 4. - Concluded.

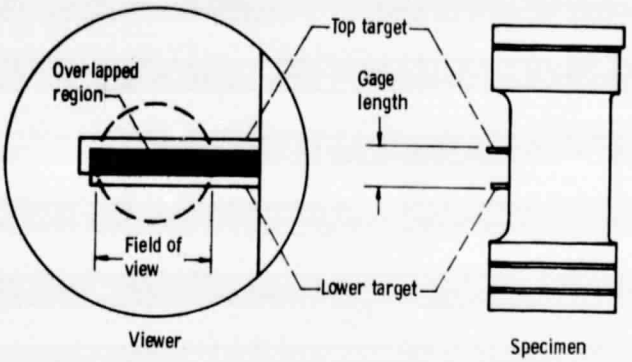

Figure 5. - Schematic of superimposed target image in viewer for backlighted targets.

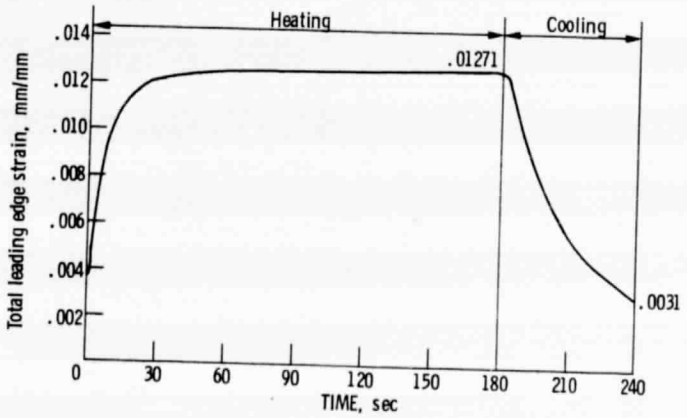

Figure 6. - Total leading edge strain for simulated turbine blade of B-1900 alloy.